Extremely slow carbon diffusion in carbon-supersaturated surface of ferrite

J. Čermák*, L. Král

Institute of Physics of Materials, v.v.i., AS CR, CEITEC IPM, Žižkova 22, 616 62 Brno, Czech Republic

Abstract

Carbon diffusion was studied in carbon-supersaturated surface layer of commercial ferrite-martensite Cr-Mo steel P91 and in two model ferrite materials: in pure α-Fe, and in ferrite Fe-Cr alloy. The carbon surface layer, the thickness of which was about 40 nm, was physical-vapor-deposited and isothermal diffusion anneals were carried out at selected temperatures between 573 K and 1073 K. The depth profiles of carbon were measured by SIMS. It was found that the carbon diffusion proceeded much more slowly in carbon-supersaturated surfaces than in matrices with equilibrium carbon concentration. The carbon diffusion coefficients obtained, D, were close to literature values reported for C diffusion in carbide phase. Measured values of D in pure α-Fe, α-Fe-Cr and P91 steel above 773 K were identical. However, significantly higher values of D were measured in P91 below the temperature of 773 K, which was ascribed to different mobility of substitution elements.

1. Introduction

Carbon supersaturation in iron-based matrices is encountered in many advanced materials either in the bulk or close to protective carbon-containing surface layers. Small carbon atoms can occupy the tetragonal or the octahedral interstitial sites in the lattice. It was, however, shown that the octahedral sites are much more preferred [1, 2]. It is known that C-C interaction energy is positive. Its high value of about 150 kJ mol^{-1} estimated in [3] indicates a strong repulsion of C-C nearest neighbors. This repulsion apparently contradicts any clustering of C atoms that might lead to carbon-supersaturation. However, relaxation measurements and calculations [4, 5] have proved that complexes or even clusters of carbon atoms must exist. It has been shown that relatively numerous vacancies or iron atom mediated di-carbon, tri-carbon and more complex clusters can be sufficiently stable [3, 6, 7]. Carbon-supersaturation has been observed in an astonishingly large extent. The actual carbon-supersaturation attainable in BCC Fe can reach a level of up to about 16 at.% [8].

It can be intuitively expected that the carbon atoms in clusters move by a co-ordinate collective mechanism [3, 9] and that their mobility is lower than the mobility of a single interstitial carbon atom. This was confirmed by means of a computer simulation [10–13]. In [11], it was shown that carbon diffusion in ferrite decreases with increasing carbon concentration. The authors of [8] estimated the ratio of the carbon diffusion coefficient in equilibrium and in carbon-supersaturated lattice at room temperature of as high as 10^6. Extended carbon clusters and transient carbides were directly observed [14–18].

Another instance, in which the carbon diffuses in a carbon-supersaturated matrix, can be encountered during the decay of ferrite-martensite structures [19]. Details of the bainite reaction that involved the decay of supersaturated bainitic ferrite were thoroughly investigated in a number of studies [14, 19–24].

Carbon diffusion in carbon-supersaturated ferrite (-martensite) lattice also governs the production of a new type of bainite steels utilizing the quenching and partitioning (Q&P) technique [25–27].

Carbon diffusion in ferrite Fe-Cr-X-C materials

---

*Corresponding author: tel.: +420 532 290 422; fax: +420 541 218 657; e-mail address: cermak@ipm.cz

with equilibrium lattice carbon concentration (lower than carbon solution limit), were studied, e. g., in [28–34]. Majority of published data were obtained by diffusion couple technique [28–30, 34]. Co-diffusion of C and N was investigated in [31], the work [32] was focused to redistribution of carbon and substitution constituents close to the free surface.

It can be summarized that the carbon diffusion in carbon-supersaturated ferrite matrices governs technologically important processes, but the carbon diffusion itself in carbon-supersaturated matrices is not fully understood. Up to the knowledge of the present authors, the only rough estimation of the carbon diffusion coefficient D at room temperature in carbon-supersaturated ferrite was published in [8].

In the present paper, carbon diffusion coefficients were measured in the carbon super-saturated surface layer on commercial steel P91 designed for application in power engineering at temperatures up to 923 K. To separate the influence of its chemical composition, the measurements were carried out also in two model carbon-coated materials: in Fe and Fe-Cr alloy.

2. Experimental

2.1. Samples preparation

Commercial P91 ferrite-martensite chromium steel (0.10 C, 0.40 Mn, 8.5 Cr, 0.10 Ni, 0.88 Mo, 0.23 V, 0.10 Nb, 0.045 N, bal. Fe, all in wt.%) was purchased, model materials Fe and ferrite Fe-Cr binary alloy (Fe-15.17wt.%Cr) were prepared from pure elements by induction melting in Ar (purity 6N) and casting in a Cu mould. Purity of Fe and Cr was 99.995 % and 99.997 % (metal basis), respectively. The concentration of interstitials was following: C – 44 ppm (obtained by C-IR analysis), O – 34 ppm (IGF-NDIR), and N < 10 ppm, H < 5 ppm (IGF-TC). All the experimental materials were annealed at 1423 K/20 h in pure Ar before measurement. Diffusion samples (10 mm in diameter × 4 mm in height) were machined from the annealed ingots.

Carbon surface layers with a thickness of $h \sim 40$ nm were deposited by physical vapor deposition (PVD) technique. In order to increase the adherence of the carbon layer to the substrate, prior to the PVD the sample surface was etched in a mixture of $C_2H_6O : HNO_3 = 98 : 2$ for about 5 s at the room temperature.

2.2. Diffusion anneals

In order to maintain the isothermal regime even during short diffusion anneals, the samples were annealed in a special vacuum furnace ULVAC RIKO MILA-5000 with extremely intensive infra-red heat-

ing in a vacuum of about 5×10^{-6} mbar. The diffusion time, t, varied between a few minutes to hundreds of hours. Both the heating and cooling were very rapid (hundreds of Kelvins in the first few seconds at the beginning and the end of the annealing). The t values at the highest diffusion temperatures were corrected to take into account the heating-up and cooling-down times. Diffusion temperatures were chosen in the interval between 573 and 1073 K and were stabilized within ± 0.1 K.

During the diffusion anneals, a carbon-supersaturated region was created in the vicinity of the original free surface. The annealing was conducted in paraequilibrium [35] conditions. The substitution elements were *frozen* and no layer/substrate interface reaction occurred and, therefore, no carbide phase was present. Analogous situation (carbon supersaturation without carbide precipitation) is known at so-called *Low-Temperature Colossal Carbon Supersaturated* surfaces of austenitic steels investigated [36].

2.3. Measurement of relative carbon concentration

Measurements were done utilizing SIMS technique (MiniSIMS Millbrook equipped with depth profiling module and with a quadrupole mass spectrometer). A focused beam of accelerated Ga^+ ions oriented perpendicular to the sample surface was used for the sputtering-off in the selected square area of the surface of the sample. The total number of charged sputtered-off carbon-containing fragments with the chosen ratio of the mass to the charge (m/e) was registered during sputtering-off scans, each of which removed one plane parallel layer. This number of fragments were taken for the relative carbon concentration, c_C, in the respective layer.

In Fig. 1, a section of mass spectra is plotted showing the lines of lightest carbon-containing negative-charged secondary fragments. The figure illustrates the difference between the spectra obtained with P91 sample without carbon layer and with the sample covered by carbon layer in the state before anneal. It is shown that there are five channels ($m/e = 12$, 13, 24, 25 and 26) that are suitable for carbon detection. It is also evident that the signals at channels $m/e = 13$, 25, 26 are influenced by other interstitials (H, N). It was found that also signal at $m/e = 24$ was considerably influenced by oxygen concentration, which might also negatively affect the measurement of carbon concentration. Therefore, all measurements in the present work were carried out using the channel $m/e = 12$ despite the fact that this channel is not the most intensive one. To avoid the edge-effects, only counts recorded in the central part $60 \times 60 \, \mu m^2$ of the crater area (total area was $100 \times 100 \, \mu m^2$) were accepted as counts that con-
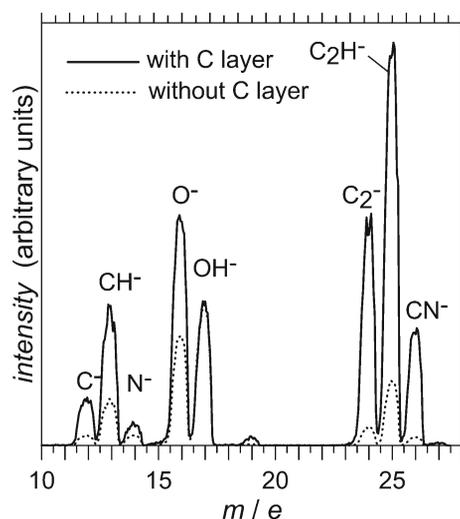
Fig. 1. XRD pattern with the lightest carbon-containing negative fragments. Measured with P91 without PVD carbon layer (dotted line) and after the carbon deposition (solid line).

Fig. 2. Profile of sputter crater measured by AFM using Fe sample after 1000 sputter scans. x and y, the depth and the lateral co-ordinate parallel with the surface, respectively.

tributed to the true value of c_C in the respective layer.

2.4. Calibration of the penetration depth

To calibrate the depth co-ordinate x of measured depth profiles (DPs), relation between the serial number of each sputtered layer and the corresponding depth x beneath the original surface was found. After a known number of sputter scans the depth of the sputter crater was measured using the con-focal microscope Olympus LEXT OLS3100 with an AFM module. The profile of the crater edge after 1000 sputter scans is shown in Fig. 2, where x and y stand for the depth and lateral co-ordinate parallel to the surface, respectively. Repeated measurement of the profile of the sputtered-off step at different selected positions along the crater rim showed an average total difference of $\Delta x = (2.86 \pm 0.09) \times 10^{-7}$ m between the original free surface and the crater bottom, which resulted in a calibration factor of $f_x = (0.29 \pm 0.08)$ nm per one sputtered layer.

2.5. Measurement of carbon concentration depth profiles

The DPs were measured both before ($t = 0$), and after each diffusion anneal at six diffusion temperatures T. Typical maximum sputtered depth was 100 nm. Repeating the sputtering scan (depth profiling procedure) produced a depth dependence of c_C. In Figs. 3, 4, typical DPs are exemplified by profiles obtained with a pure Fe sample. The curves $c_C(x)$ in Fig. 4 are plotted after the correction for the back-

ground. It can be seen that the depth dependence of the carbon concentration showed well-defined surface layer, the chemical composition of which at $t = 0$ approached 100 % C. The minimum quantity of $c_C(x)$ observed at the very beginning of the sputter process (at low values of x) is a consequence of the surface contamination by adsorbed impurity atoms and the transient regime at the commencement of the sputter process [37]. Departure of $c_C(x)$ from an ideal rectangular shape at $t = 0$ (i.e., constant carbon concentration $c_C(x) = c_0$ within the deposited surface layer of thickness h, and then the abrupt drop of $c_C(x) = 0$ at $x = h$) is caused by non-stable PVD and by the statistical character of sputtering process.

3. Results and discussion

3.1. Evaluation of data

The experimental arrangement of the current carbon diffusion study was chosen so that the observed carbon concentration $c_C(x, t)$ could be described by a known analytical solution derived for the case of diffusion from the surface layer of thickness h into a half-space [38].

The shaded area a_{exp} beneath the DP curve (see Fig. 3), proportional to the quantity of the carbon atoms in the surface layer, decreased with increasing diffusion time t as is obvious in Fig. 4. Since the carbon vapor pressure at diffusion temperatures [39] was always much lower than the residual pressure in the vacuum chamber during each anneal, the decrease in a_{exp} cannot be ascribed to carbon evaporation. Also
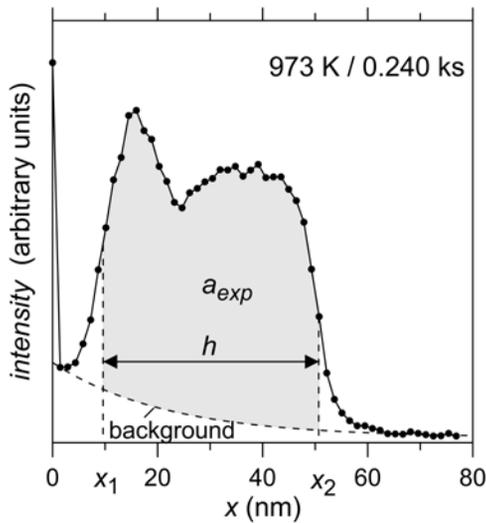
Fig. 3. Example of measured DP measured using Fe sample after diffusion annealing at 973 K/0.24 ks.
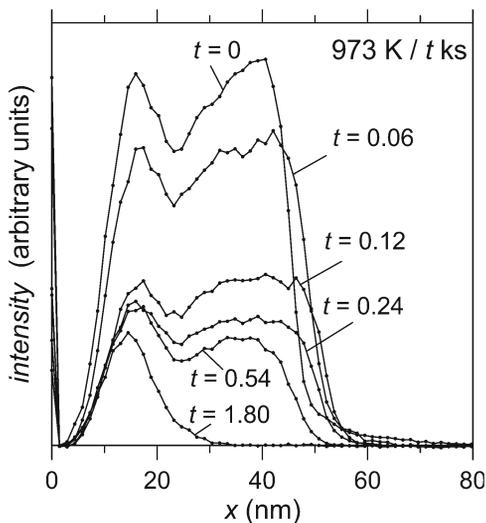
Fig. 4. Examples of measured DPs measured using Fe sample after diffusion annealing at 973 K for diffusion times up to $t_{max} = 1.80$ ks. DPs are corrected for background.

a decrease in a_{exp} caused by a reaction of the carbon deposited on the sample surface with the residual oxygen in the chamber can be excluded. Repeating similar diffusion experiments using copper samples (Cu dissolves much less carbon than α-Fe does) resulted in time-independent values of a_{exp}. Hence, it can be concluded that the rate of decrease of $a_{exp}(t)$ with increasing t is exclusively due to carbon in-diffusion into the samples.

For the carbon layer thickness, $h = x_2 - x_1$, the average width of layer depth profiles was taken measured between the two inflection points of $c_C(x, t)$ (Fig. 3).
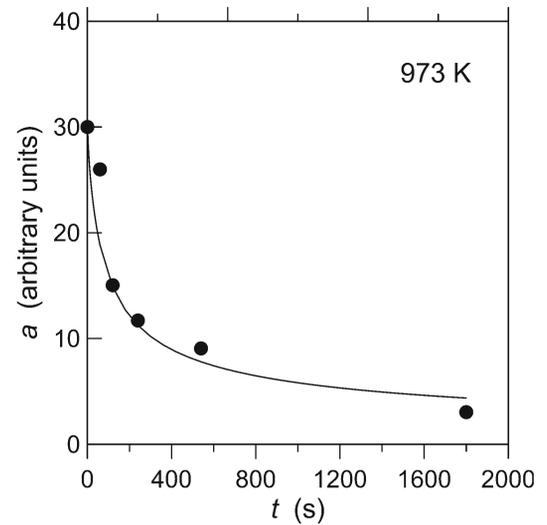
Fig. 5. Example of time dependence of a measured using Fe sample. Annealed at 973 K for times up to $t_{max} = 1.80$ ks. Full points – experimental values of a_{exp}, solid line (see Eq. (2).)

The decrease in a_{exp} was the only significant and well defined change of DPs with increasing t observed, because concentration tails of $c_C(x, t)$ measured in greater depths $x > h$, were too flat to be used for reliable evaluation of D using SIMS. As an analogy to Borisov's surface-decay method [40], an analytical expression describing the relation between a and t can be obtained. Assuming that the concentration of diffusing species from the surface layer of thickness h into a half-space is defined by the equation [38]:

$$c_C = \frac{1}{2}c_0 \left\{ \mathrm{erf}\left(\frac{h-x}{2\sqrt{Dt}}\right) + \mathrm{erf}\left(\frac{h+x}{2\sqrt{Dt}}\right) \right\}, \quad (1)$$

the total amount of carbon in the surface layer, a, can be obtained by its integration with respect to x within the layer of thickness h. The result reads:

$$a = \int_{x_1}^{x_2} c_C \mathrm{d}x = \quad (2)$$

$$= c_0 \left\{ h\, \mathrm{erf}\left(\frac{h}{\sqrt{Dt}}\right) + \sqrt{\frac{Dt}{\pi}} \left[\exp\left(-\frac{h^2}{Dt}\right) - 1 \right] \right\}.$$

Equation (2) was fitted to experimental values of $a_{exp}(t)$ and D's were obtained as fitting parameters. For the value of a_{exp}, shaded area beneath the c_C curve was calculated by numerical integration as illustrated in Fig. 3, and value of h was considered as known parameter for the optimization carried out with the help of *TableCurve 2D* SW package [41]. An illustrative example of time dependence $a_{exp}(t)$ is shown in Fig. 5.

T a b l e 1. Carbon diffusion coefficients D obtained for diffusion times from 0 to t_{max}

	Material							
	Fe		Fe electropolished		Fe-Cr		P91	
T (K)	D (m^2 s^{-1})	t_{max} (ks)	D (m^2 s^{-1})	t_{max} (ks)	D (m^2 s^{-1})	t_{max} (ks)	D (m^2 s^{-1})	t_{max} (ks)
1073	1.5×10^{-16}	0.180	9.8×10^{-17}	0.840	1.0×10^{-16}	0.180	1.9×10^{-16}	0.240
973	4.9×10^{-17}	1.80	3.8×10^{-17}	0.960	2.4×10^{-17}	0.600	2.1×10^{-17}	1.32
873	1.7×10^{-18} 3.2×10^{-18}	2.88	3.8×10^{-18} 3.4×10^{-18}	1.44	3.2×10^{-18}	0.900	3.2×10^{-18}	1.80
773	8.2×10^{-20}	3.54	1.3×10^{-19}	68.4	6.5×10^{-20}	10.8	6.5×10^{-19}	3.60
673	7.1×10^{-21}	205	4.3×10^{-21}	436	3.6×10^{-21}	540	4.1×10^{-19} 9.5×10^{-19}	72.0
573							2.6×10^{-21} 1.4×10^{-21}	403

Fig. 6. Carbon diffusion coefficients D in carbon-supersaturated ferrite matrix. Dotted lines – prediction limits at level 95 % confidence, solid line – Arrhenius equation.

3.2. Carbon diffusion coefficients and comparison with literature

All the calculated values of D are listed in Table 1. Their numerical uncertainty originates from the location of the crater on the sample surface and from the fitting errors. Interval $(D \times 1/2; D \times 2)$ can be taken as the most likely interval of calculated values of D that reasonably counts for the disturbing factors. This estimation of the experimental error of D complies well with the observed differences in D obtained when some of the experiments were repeated (see, e.g., Fe at 873 K, alloy P91 below 773 K).

3.2.1. Carbon diffusion in Fe

The results obtained with the mechanically polished samples of α-Fe (careful mechanical polishing finished with a fine diamond paste) are plotted in Arrhenius diagram in Fig. 6 – see full points. Depth profiles $c_C(x, t)$ were measured from the surface down to a typical depth of $x_{max} \sim 100$ nm. This is a region that may be influenced by metallographic polishing. For this reason, the measurement of D was repeated with Fe samples finished by electrolytic polishing in a mixture $CH_3COOH : HClO_4 = 9 : 1$, $40\,V\,1^{-1}\,min^{-1}$. In this manner, the surface layer with a thickness of about 25 μm was removed that might be influenced by mechanical treatment (the Beilby layer [42]). Repeated measurement using samples that have been electrolytically polished prior to PVD of carbon provided values of D that are also plotted in Fig. 6 (the open points). It is clear that the results are identical with those obtained using mechanically finished samples. After this test that revealed independence of D on the type of surface finishing, experiments with other materials were carried out solely using mechanically finished samples.

3.2.2. Carbon diffusion in Fe-Cr

It is known that there is a strong affinity between carbon and chromium that leads to the formation of stable chromium carbides [43]. Therefore, Fe-Cr alloy was prepared to test the influence of Cr on carbon diffusion in supersaturated ferrite matrix. Carbon content in the alloy in as-prepared state was negligible (see the purity of starting materials given above) and the measurement of DPs in a carbon-supersaturated state was carried out during very early stages of carbon in-diffusion from the surface layer into the bulk of the substrate. Under such conditions, the atoms of the substitution elements cannot respond to the car-

bon atoms flooding the subsurface region. They are effectively *frozen* and no carbide phase can be present in the diffusion zone to a considerable extent.

These results can be seen in Fig. 6 (open squares). It is obvious that the carbon diffusion coefficients are equal to the values obtained for pure Fe – no retarding effect of Cr was observed. It seems that carbon in carbon-supersaturated ferrite matrix of a Fe-based alloy does not depend on the presence of the strong carbide former substitution atoms.

In Fig. 6 it can be seen that the temperature dependence of D is linear – within the frame of experimental error estimated – in coordinates log D vs. $1/T$, which enables one to evaluate parameters in the Arrhenius equation $D = D_0 \exp(-\Delta H/RT)$ (R is gas constant). The enthalpy $\Delta H = (158 \pm 5)\,\mathrm{kJ\,mol^{-1}}$ and frequency factor $D_0 = 10^{-(8.11\pm0.30)}\,\mathrm{m^2\,s^{-1}}$ obtained by fitting Arrhenius equation to the entire data set (mechanically and electrolytically finished Fe samples and Fe-Cr samples) adequately describe carbon diffusion in supersaturated surface. The dotted lines in Fig. 6 show the prediction limits of D at a 95 % probability level.

3.2.3. Carbon diffusion in P91

Prior to the diffusion measurement, the alloy P1 was austenitized by annealing at 1423 K for 20 h in silica tube filled with pure Ar (5N6) and then air cooled. Original structure [44, 45] changed after this thermal pre-treatment to ferrite (martensite with a very low degree of tetragonality [46]). XRD and EBSD analyses showed that the content of carbides was negligible: traces of Cr_7C_3 and Hägg carbide Fe_5C_2 were revealed by XRD only. The presence of carbide $M_{23}C_6$ was excluded. The content of retained austenite was very low, about 0.3–0.5 wt.%.

The Arrhenius diagram of carbon diffusion coefficients is plotted in Fig. 7 (the full points). It can be seen that the temperature dependence of D breaks down into two distinct branches (see solid lines in Fig. 7). At temperatures above 800 K, D's were very low, below the temperature of about 700 K, the obtained values of D were significantly higher than the extrapolation of high temperature data.

We propose the following explanation of different temperature dependence of the carbon diffusion coefficient in ferrite materials Fe and Fe-Cr on one hand, and P91 with the break between temperatures 700 K and 800 K on the other. It is based on different mobility of substitution elements in both temperature regions and on different carbon concentration, which makes as much as two orders of magnitude (about 44 ppm C in Fe and Fe-Cr and about 0.4 at.% C in P91 – see paragraph 2.1). At higher temperatures, the mobility of substitution elements is higher and hence, there is a great number of the carbon Fe-M-C clusters (pre-
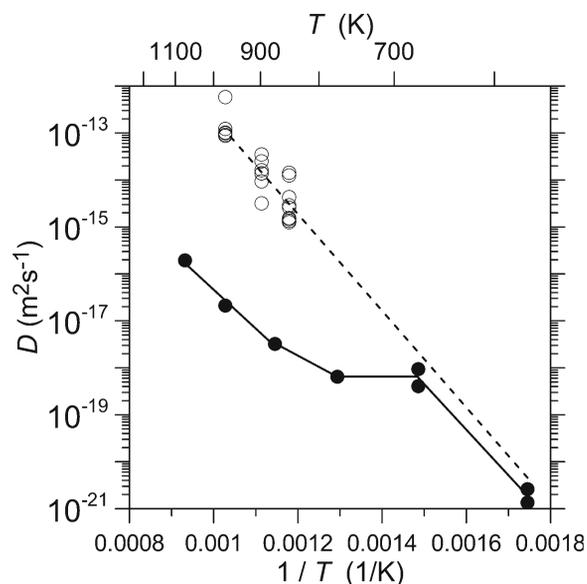
Fig. 7. Carbon diffusion coefficients D in carbon-supersaturated matrix of P91. Full points and solid lines – present work, open points – literature data [34], dashed line – low temperature extrapolation of data from [34].

-nucleation carbide centers) that act as effective traps for carbon atoms. At lower temperatures, on the other hand, the carbon atoms in P91 move as almost free interstitials through the matrix with not so numerous effective traps. Different low-temperature carbon diffusivity in P91 compared to that in other ferrite materials (Fe and Fe-Cr) (cf. Figs. 6 and 7) is caused most likely by different carbon atom concentration in the lattice of materials under study, since relatively high carbon concentration in P91 saturates partly the carbon traps and, in average, decreases their efficiency. This is not the case of other ferrite materials, where the pre-nucleation centers are not so saturated and, therefore, their stopping efficiency for carbon atoms diffusing from the surface is higher.

This explanation can be confirmed by comparing the current results with literature data obtained using samples containing equilibrium carbon concentration in the lattice. If we plot the literature values of D_{eq} from [34] obtained for P91 at much higher temperatures and after much longer diffusion times (10–5000 h) – i.e., in *non-supersaturated* state – we can see that the current low-temperature values of D are reasonably consistent with the low-temperature extrapolation of literature values of D_{eq} from [34] (dashed line in Fig. 7).

3.2.4. Comparison with literature

The current results are plotted in Fig. 8 together with the literature data reported for C diffusion in α-Fe (for review of these, see, e.g., in [47]), in
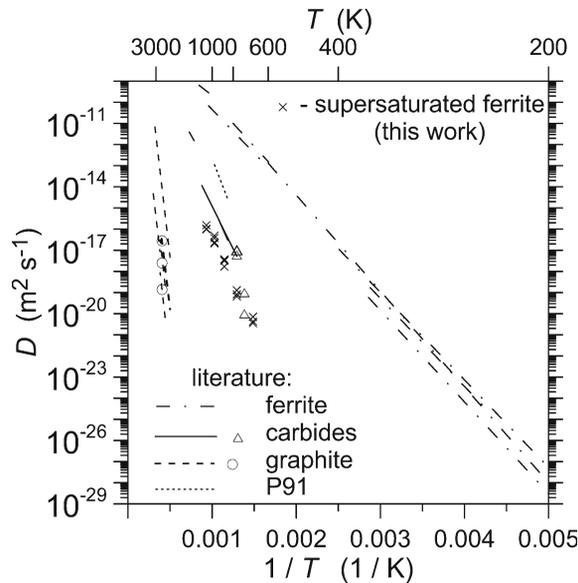
Fig. 8. Arrhenius diagram of carbon diffusion coefficients. Literature data: ferrite (for review – see in [47], carbides [48–56], graphite [57–62], P91 [34]).

carbides [48–56], in P91 [34] and in graphite [57–62].

It is obvious that the present values of D are much lower than the D's reported in the literature for an equilibrium carbon concentration in matrix and higher than the C diffusion in graphite. They are close to the carbon diffusion coefficients reported for carbide phases (in Fe_3C [48–56] and in Hägg carbide Fe_5C_2 [56]) even if no carbide phase in significant amount was present in the materials under study (tested by XRD and EBSD). This may be caused by the fact that carbon atoms in a supersaturated ferrite matrix are strongly influenced by pre-carbide coupling with their neighbors and their collective movement is considerably constrained.

4. Conclusions

In the present work, the carbon diffusion coefficient, D, in carbon-supersaturated surface of ferrite lattice of P91 was measured. Measurement was carried out in the temperature interval between 573 K and 1073 K by depth profiling using Ga^+ sputtering-off. Secondary mass spectroscopy was utilized as analytical method for carbon concentration measurement. It was found that:

(i) The carbon diffusion rate in a carbon-supersaturated state is very slow as compared to carbon diffusion in non-supersaturated matrix. This experimental fact supports previous estimates of D [8]. It was found that the carbon diffusion in carbon-supersaturated ferrite can be described by Arrhe-

nius equation $D = 10^{-(8.11\pm0.30)} \times \exp[-(158 \pm 5)$ $kJ\,mol^{-1}/RT]\,m^2\,s^{-1}$.

(ii) The values of D obtained in the present work above 800 K are close to the values published in the literature for the carbon diffusion coefficient in carbide phase.

(iii) It follows from items (i and ii) that the carbon atoms in carbon-supersaturated state diffuse in relatively ordered structures. The ordered formations, however, are not carbide nuclei, because

(iv) the values of D in the carbon-supersaturated ferrite matrix are not dependent on the presence of chromium atoms that act as strong carbide formers.

(v) Above 800 K, D's in P91 are close to values obtained in Fe and Fe-Cr and are much lower than D_{eq}. Below the temperature 700 K, the values of D approach D_{eq}.

References

[1] Domain, C., Becquart, C. S., Foct, J.: Phys. Rev. B, *69*, 2004, p. 144112. doi:10.1103/PhysRevB.69.144112
[2] Jiang, D. E., Carter, E. A.: Phys. Rev. B, *67*, 2003, p. 214103. doi:10.1103/PhysRevB.67.214103
[3] Bhadeshia, H. K. D. H.: J. Mater. Sci., *39*, 2004, p. 3949. doi:10.1023/B:JMSC.0000031476.21217.fa
[4] Johnson, R. A.: Acta Metall., *15*, 1967, p. 513. doi:10.1016/0001-6160(67)90084-3
[5] Keefer, D., Wert, C.: J. Phys. Soc. of Japan, *18*, 1963, p. 110.
[6] Forst, C., Slycke, J., Van Vliet, K. J., Yip, S.: Phys. Rev. Let., *96*, 2006, p. 175501. doi:10.1103/PhysRevLett.96.175501
[7] Vehanen, A., Hautojarvi, P., Johansson, J., Yli-Kauppila, J., Moser, P.: Phys. Rev. B, *25*, 1982, p. 762. doi:10.1103/PhysRevB.25.762
[8] Weck, A., Sinclair, C. W., Scott, C. P., Maunder, C.: J. Mater. Sci., *47*, 2012, p. 6939. doi:10.1007/s10853-012-6641-6
[9] Ishii, A., Li, J., Ogata, S.: PLOS ONE, *8*, 2013, e60586. doi:10.1371/journal.pone.0060586
[10] Tapasa, K., Barashev, A. V., Bacon, D. J., Osetsky, Yu, N.: Acta Mater., *55*, 2007, p. 1. doi:10.1016/j.actamat.2006.05.029
[11] Kabir, M., Lau, T. T., Lin, X., Yip, S., Van Vliet, K. J.: Phys. Rev. B, *82*, 2010, p. 134112. doi:10.1103/PhysRevB.82.134112
[12] Johnsson, R. A., Dienes, G. J., Damask, A. C.: Acta Metall., *12*, 1964, p. 1215. doi:10.1016/0001-6160(64)90105-1

[13] Ishii, A., Ogata, S., Kimizuka, H., Li, J.: Phys. Rev. B, *85*, 2012, p. 064303.

[14] Caballero, F. G., Miller, M. K., Garcia-Mateo, C., Capdevila, C., Babu, S. S.: Acta Mater., *56*, 2008, p. 188. doi:10.1016/j.actamat.2007.09.018

[15] Faraoun, H. I., Zhang, Y. D., Esling, C., Aourag, H.: J. Appl. Phys., *99*, 2006, p. 093508. doi:10.1063/1.2194118

[16] Koeniger, A., Hammerl, C., Zeitler, M., Rauschenbach, B.: Phys. Rev. B, *55*, 1997, p. 8143. doi:10.1103/PhysRevB.55.8143

[17] Deng, C. M., Huo, C. F., Bao, L. L., Shi, X. R., Li, Y. W., Wang, J., Jiao, H.: Chem. Phys. Letters, *448*, 2007, p. 83. doi:10.1016/j.cplett.2007.09.055

[18] Clarke, A. J., Speer, J. G., Miller, M. K., Hackenberg, R. E., Edmonds, D. V., Matlock, D. K., Rizzo, F. C., Clarke, K. D., De Moor, E.: Acta Mater., *56*, 2008, p. 16. doi:10.1016/j.actamat.2007.08.051

[19] Fielding, L. C. D.: Mater. Sci. Technol., *29*, 2013, p. 383. doi:10.1179/1743284712Y.0000000157

[20] Li, H. Y., Lu, X. W., Wu, X. C., Min, Y. A., Jin, X. J.: Mater. Sci. Eng. A., *527*, 2010, p. 6255. doi:10.1016/j.msea.2010.06.045

[21] Kang, M. K., Ai, Y. L., Zhang, M. X., Yang, Y. Q., Zhu, M., Chen, Y.: Mater. Chem. Phys., *118*, 2009, p. 438. doi:10.1016/j.matchemphys.2009.08.014

[22] Zhong, N., Wang, X. D., Wang, L., Rong, Y. H.: Mater. Sci. Eng. A, *506*, 2009, p. 111. doi:10.1016/j.msea.2008.11.014

[23] Van Bohemena, S. M. C., Santofimia, M. J., Sietsma, J.: Scripta Mater., *58*, 2008, p. 488. doi:10.1016/j.scriptamat.2007.10.045

[24] Lawrynowicz, Z., Dymski, S.: Advances in Materials Sci., *8*, 2008, p. 80.

[25] Edmonds, D. V., He, K., Rizzo, F. C., De Cooman, B. C., Matlock, D. K., Speer, G. J.: Mater. Sci. Eng. A, *438–440*, 2006, p. 25. doi:10.1016/j.msea.2006.02.133

[26] Ernst, F., Cao, Y., Michal, G. M.: Acta Mater., *52*, 2004, p. 1469. doi:10.1016/j.actamat.2003.11.027

[27] Tsuchiyama, T., Tobata, J., Tao, T., Nakada, N., Takaki, S.: Mater. Sci. Eng. A, *532*, 2012, p. 585. doi:10.1016/j.msea.2011.10.125

[28] Sopoušek, J., Million, B.: Kovove Mater., *41*, 2003, p. 118.

[29] Million, B., Foret, R., Rek, A., Stránský, K.: Kovove Mater., *37*, 1999, p. 314.

[30] Million, B., Michalička, P., Stránský, K.: Kovove Mater., *36*, 1998, p. 281.

[31] Pilous, V., Stránský, K., Kučera, J., Milion, B., Drybčák, P., Rek, A.: Kovove Mater., *29*, 1991, p. 31.

[32] Pokorná, A., Million, B., Vřešťál, J., Stránský, K., Patoka, V.: Kovove Mater., *29*, 1991, p. 348.

[33] Kučera, J., Hajduga, M.: Kovove Mater., *37*, 1999, p. 303.

[34] Foret, R., Million, B., Svoboda, M., Stránský, K.: Sci. and Technol. of Welding and Joints, *6*, 2001, p. 405.

[35] Michal, G. M., Ernst, F., Heuer, A. H.: Metal. Mater. Trans. A, *37*, 2006, p. 1819. doi:10.1007/s11661-006-0124-9

[36] Cao, Y., Ernst, F., Michal, G. M.: Acta Mater., *51*, 2003, p. 4171. doi:10.1016/S1359-6454(03)00235-0

[37] Vickerman, J. C., Gilmore, I. S.: Surface Analysis – Principal Techniques. 2nd edition. Chichester, J. Willey and Sons 2009. doi:10.1002/9780470721582

[38] Crank, J.: The Mathematics of Diffusion. Oxford, Clarendon Press 1957.

[39] http://www.powerstream.com/vapor-pressure.htm (Juni 2013).

[40] Borisov, V. T., Golikov, V. M., Ljubov, B. Y., Sherbedinsky, G. V.: In: Proceeding of the International Conference – Research with Radioisotopes in Physics and Industry. Ed.: Extermann, R. C. Oxford, Pergamon Press 1958, p. 212.

[41] TableCurve 2D Automated Curve Fitting & Equation Discovery, 5.01 for Windows SYSTAT Software Inc., 501 Canal Boulevard, Suite F, Richmond, CA 94804-2028.

[42] Rokicki, R., Hriniewicz, T.: Trans. Institute of Metal Finishing, *90*, 2012, p. 188. doi:10.1179/0020296712Z.00000000031

[43] Villars, P., Prince, A., Okamoto, H.: Handbook of Ternary Phase Diagrams 1.0. Materials Park, The Materials Information Society 1997 (CD ROM).

[44] Coleman, K. K., Newell Jr., W. F.: Welding Journal, *86*, 2007, p. 29.

[45] Czyrska-Filemonowicz, A., Zielinska-Lipiec, A., Ennis, P. J.: J. Achievements Mater. Manufact. Eng., *19*, 2006, p. 43.

[46] Von Hagen, I., Bendick, W.: In: Niobium, Science & Technology: Proceedings of the International Symposium Niobium 2001. Eds.: von Hagen, I., Bendick, W., Orlando, FL, Niobium 2001 Ltd. 2002, p. 753.

[47] Landolt, H. Börnstein, R.: Numer. Data and Functional Relationships in Sci. and Technol., Group III: Crystal and Solid State Physics, vol. 26, Diffusion in Solid Metals and Alloys. Ed.: Mehrer, H. Berlin-Heidelberg-New York-Paris-Tokyo-Hong Kong-Barcelona, Springer Verlag 1990.

[48] Levchenko, E. V., Evteev, A. V., Belova, I. V., Murch, G. E.: Acta Mater., *57*, 2009, p. 846. doi:10.1016/j.actamat.2008.10.025

[49] Levchenko, E. V., Evteev, A. V., Belova, I. V., Murch, G. E.: Defect and Diffusion Forum, *283–286*, 2009, p. 24. doi:10.4028/www.scientific.net/DDF.283-286.24

[50] Young, D., Zhang, J.: In: High Temperature Corrosion and Materials Chemistry 7. Eds.: Wuchia, E., Opila, E., Fergus, J., Maruyama, T., Shifler, D. New Jersey, Electrochemical Society 2009, p. 3.

[51] Ozturk, B., Fearing, V. L., Ruth, J. A., Simkovich, G.: Metall. Trans. A, *13*, 1982, p. 1871. doi:10.1007/BF02647845

[52] Ozturk, B., Fearing, V. L., Ruth, J. A., Simkovich, G.: Solid State Ionics, *12*, 1984, p. 145. doi:10.1016/0167-2738(84)90141-3

[53] Kofstad, P.: Selected topics in high temperature Chemistry. Eds.: Johannesen, Ø., Andersen, A. G. New York, Elsevier Science Publishers 1989.

[54] Schneider, A., Inden, G., Grabke, H. J.: Interface controlled materials (EUROMAT 99). Eds.: Rühle, M., Gleiter, H. Weinheim, Wiley-VCH 2000.

[55] Hillert, M., Hägland, L., Ågren J.: J. Appl. Phys., *98*, 2005, p. 053511. doi:10.1063/1.1999833

[56] Schneider, A., Inden, G.: Calphad, *31*, 2007, p. 141. doi:10.1016/j.calphad.2006.07.008

[57] Kanter, M. A.: Phys. Rev., *107*, 1957, p. 655. doi:10.1103/PhysRev.107.655

[58] Evans, R. B., Love, L. D., Kobisk, E. H.: J. Appl. Phys., *40*, 1969, p. 3058. doi:10.1063/1.1658132

[59] Feates, F. S.: J. Nucl. Mater., *27*, 1968, p. 325. doi:10.1016/0022-3115(68)90091-3

[60] Hennig, G. R.: J. Chem. Phys., *42*, 1965, p. 1167. doi:10.1063/1.1696098

[61] Sach, R. S., Williams, W. J.: Carbon, *12*, 1974, p. 425. doi:10.1016/0008-6223(74)90008-6

[62] Adda, Y., Philibert, J.: La Diffusion dans les Solides. Vol. II. Paris, Saclay, INSTN, Presses universitaires de France 1966, p. 1166 (in French).